



HAL
open science

Fate of nanoplastics in the environment: Implication of the cigarette butts

Hind El Hadri, Jesus Maza Lisa, Julien Gigault, Stephanie Reynaud, Bruno Grassl

► **To cite this version:**

Hind El Hadri, Jesus Maza Lisa, Julien Gigault, Stephanie Reynaud, Bruno Grassl. Fate of nanoplastics in the environment: Implication of the cigarette butts. *Environmental Pollution*, 2021, 268, pp.115170. 10.1016/j.envpol.2020.115170 . insu-02899294

HAL Id: insu-02899294

<https://insu.hal.science/insu-02899294>

Submitted on 15 Jul 2020

HAL is a multi-disciplinary open access archive for the deposit and dissemination of scientific research documents, whether they are published or not. The documents may come from teaching and research institutions in France or abroad, or from public or private research centers.

L'archive ouverte pluridisciplinaire **HAL**, est destinée au dépôt et à la diffusion de documents scientifiques de niveau recherche, publiés ou non, émanant des établissements d'enseignement et de recherche français ou étrangers, des laboratoires publics ou privés.

Journal Pre-proof

Fate of nanoplastics in the environment: Implication of the cigarette butts

Hind El Hadri, Jesus Maza Lisa, Julien Gigault, Stéphanie Reynaud, Bruno Grassl



PII: S0269-7491(20)32958-4

DOI: <https://doi.org/10.1016/j.envpol.2020.115170>

Reference: ENPO 115170

To appear in: *Environmental Pollution*

Received Date: 20 April 2020

Revised Date: 30 June 2020

Accepted Date: 2 July 2020

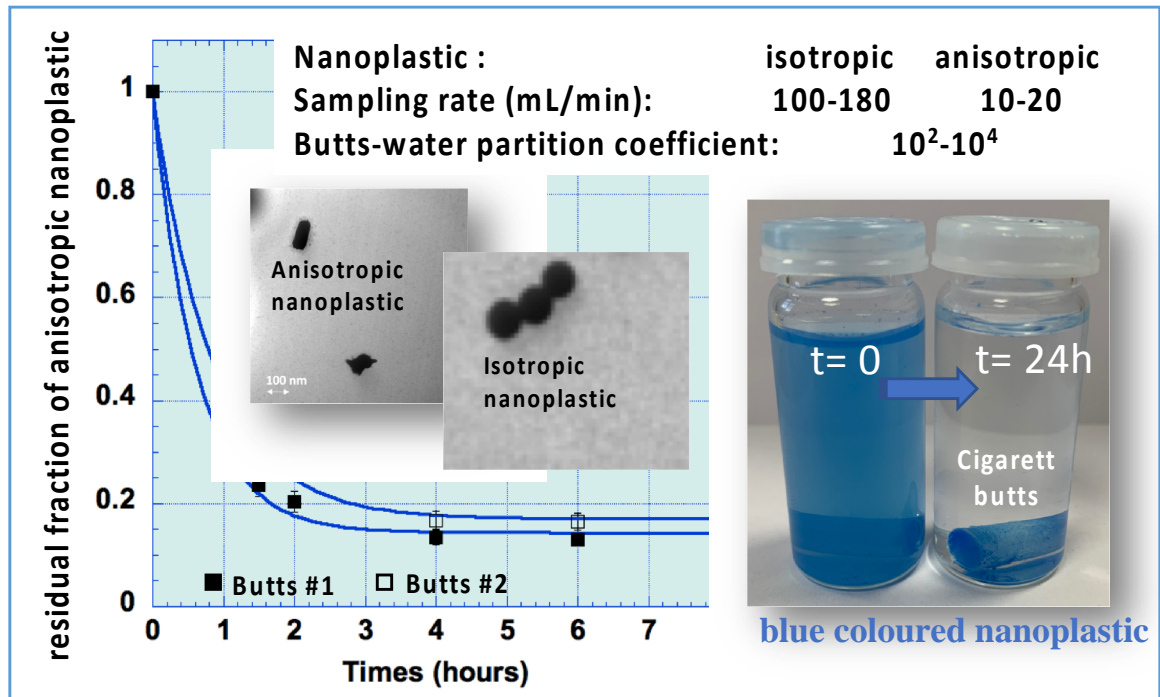
Please cite this article as: El Hadri, H., Lisa, J.M., Gigault, J., Reynaud, Sté., Grassl, B., Fate of nanoplastics in the environment: Implication of the cigarette butts, *Environmental Pollution* (2020), doi: <https://doi.org/10.1016/j.envpol.2020.115170>.

This is a PDF file of an article that has undergone enhancements after acceptance, such as the addition of a cover page and metadata, and formatting for readability, but it is not yet the definitive version of record. This version will undergo additional copyediting, typesetting and review before it is published in its final form, but we are providing this version to give early visibility of the article. Please note that, during the production process, errors may be discovered which could affect the content, and all legal disclaimers that apply to the journal pertain.

© 2020 Published by Elsevier Ltd.

Fate of nanoplastics in the environment: implication of the cigarette butts

Hind El Hadri, Jesus Maza Lisa, Julien Gigault, Stéphanie Reynaud, Bruno Grassl



Fate of nanoplastics in the environment: implication of the cigarette butts

Hind El Hadri^a, Jesus Maza Lisa,^a Julien Gigault^b, Stéphanie Reynaud^{*a}, Bruno Grassl^a

^a. CNRS/ Univ Pau & Pays Adour/ E2S UPPA, Institut des sciences analytiques et de physicochimie pour l'environnement et les matériaux, UMR 5254, 64000, Pau, France

^b. Géosciences Rennes, UMR 6118, CNRS – Université de Rennes 1, Av. Général Leclerc, Campus de Beaulieu, 35000 Rennes France

*Corresponding author: stephanie.reynaud@univ-pau.fr

Abstract: Fate, transport and accumulation of nanoplastics have attracted considerable attention in the past few years. While actual researches have been focused on nanoplastics dispersed or aggregated in different environmental systems, no study has been focused on the possibility that nanoplastics are co-transported with other natural or anthropogenic materials. Therefore, the large quantity of debris released in the environment, such as cigarette butts (CGB), could be part of the nanoplastics fate and behavior. Here we show the considerable sorption capacities of cigarette filters for nanoplastics. To address this topic, we chose polystyrene-based nanoplastics with similar state of charge (according to the physico-chemical characteristic of the zeta potential -45 to -40 mV) but with different sizes (50-800nm) and morphologies. A kinetic approach to sorption in fresh water (pH=8.05 ; $179.5 \mu\text{S cm}^{-1}$) at room temperature was carried out by means of the flow field flow analysis method (AF4) to determine the partition coefficients and water sampling rates between nanoplastics and cigarette butts. Using different models of, more or less environmentally relevant, nanoplastics (NPTs) and adequate analytical strategies, we found partition coefficients between the NPTs and CGBs ranged from 10^2 to 10^4 in freshwater conditions. We demonstrated that the physical features of the NPTs (size and morphology)

23 have an influence on the sorption behaviour. Asymmetrical shaped NPTs with broader size distribution
24 seems to be mostly retained in the CGBs after longer equilibration time. This result shows the
25 importance of the NPTs features on the mechanisms governing their transfer and fate in the
26 environment through environmental matrices, especially when other materials are involved. We
27 anticipate our work to be a starting point for investigating the co-transport of NPTs with other materials
28 present in the environment (natural and anthropogenic).

29
30 **Keywords:** nanoplastic, cigarette butts, sorption.

31
32 **Introduction**

33 Plastic pollution has attracted considerable attention from the public sector in recent years.
34 While a large majority of the relevant research has been performed on microsized plastic
35 particles, only a few groups of researchers focused their work on nanoscale plastics (Li et al.,
36 2020; Shen et al., 2019; Wagner and Reemtsma, 2019). It was now admitted that the
37 fragmentation of plastic particles releases a considerable number of nanoplastics (NPTs) (Gigault
38 et al., 2016; Hartmann et al., 2019; Lambert and Wagner, 2016a, 2016b). Similar to other classic
39 nanoparticles, NPTs may interact with various species, whether naturally present or
40 (un)intentionally released within the environment. These interactions can enhance NPT
41 transport through different natural interfaces (soil-freshwater-estuarine system-ocean) or
42 promote their accumulation in specific areas (Alimi et al., 2018; da Costa et al., 2016; Dong et al.,
43 2019).

44 Among all the types of debris found in the environment, cigarette butts (CGBs) are one of the
45 most predominant, and worldwide cigarette consumption is estimated to reach approximately 9
46 trillion by 2025 (Araújo and Costa, 2019; Mackay et al., 2002). It is estimated that more than 750
47 000 metric tons of CGBs end up as litter worldwide per year, which corresponds to
48 approximately $4.5 \cdot 10^{12}$ CGB units released into our environment each year (Novotny and
49 Slaughter, 2014). Because CGBs are composed of cellulose acetate, they can interact with
50 several organic and metallic pollutants in the environment (Chevalier et al., 2018). Pu et al.
51 recently demonstrated that CGB based-materials act as a powerful Uranium sorbent (106 mg g^{-1})
52 (Pu et al., 2019). In air, CGBs were demonstrated to sorb and release particles with different size
53 distribution (Hengstberger and Stark, 2009). In aqueous media, due to the large quantity of CGBs
54 and nanoplastics released, co-transport of NPTs and other contaminants with CGBs have to be
55 investigated for environmental and health perspectives. Indeed, NPT-CGB interaction and
56 synergy could complicate the fate and impact of both of these emergent pollutants, whose
57 behaviour is already challenging.

58 The main objective of this work is to investigate the sorption capacities of NPTs on cigarette
59 filters to evaluate the general problem of the co-transport possibility of these nanoplastics in the
60 environment. In this work, different kinds of nanoplastics were chosen. The first type of NPTs
61 tested is the one commonly used in environmental studies on the impacts of NPTs on aquatic
62 organisms and the transfer and environmental fate of NPTs. These NPTs are monodisperse and
63 spherical (Pessoni et al., 2019). On the other hand, the second type of NPTs was chosen to be
64 anisotropic and was obtained by mechanical fragmentation as described elsewhere (Davranche
65 et al., 2019; El Hadri et al., 2020; Gillibert et al., 2019). Both of these NPT series are identical in
66 terms of chemical composition (polystyrene base) and have similar surface functionality, as
67 revealed by their similar values of the zeta-potential physico-chemical parameter. A kinetic

68 approach to analyze NPT sorption on unused cigarette filters was performed, the partition
69 coefficients and mass transfer coefficients in fresh water have been evaluated.

70

71 **Materials and Methods**

72 **Reagents.** In this work, different nanoplastics have been studied: (i) commercial polystyrene
73 latex NPTs, called PSLs (certified carboxylated PSL NPTs), which are often used to study the
74 effects of nanoplastics on aquatic organisms, (Pikuda et al., 2018) and (ii) fragmented
75 polystyrene NPTs, called NPT_f, produced *via* a top-down method based on mechanical
76 degradation of primary polystyrene microplastics and recently described elsewhere (El Hadri et
77 al., 2020). The sodium nitrate used to formulate the mobile phase for the flow field-flow
78 fractionation (AF4) was purchased from Sigma-Aldrich (Darmstadt, Germany). Polyethersulfone
79 (PES) filters (0.1 μm), purchased from VWR (Fontenay-sous-Bois, France), were used to remove
80 particles from the mobile phase. All the solutions were prepared with ultrapure deionized water
81 (18.2 M Ω cm, at 25 °C) obtained from a Milli-Q system (Millipore, Molsheim, France). The
82 polystyrene latex (PSL) carboxylated beads with hydrodynamic diameters (d_H) of 50 nm, 180 nm
83 and 500 nm and blue-dyed PSLs (200 nm) were purchased from Polysciences (Hirschberg an der
84 Bergstraße, Germany). The pellets of polystyrene (PS) were purchased from Goodfellow (Lille,
85 France). The freshwater was sampled from the Gave of Pau at the location of the Laroin Bridge
86 (GPS coordinates: 43.305443, -0.436205) and presented a pH of 8.05 and a conductivity of 179.5
87 $\mu\text{S cm}^{-1}$ at 23.1 °C.

88

89 **Nanoplastic preparation.** The protocol described elsewhere has been reproduced (El Hadri et
90 al., 2020). Briefly, the fragmentation for NPT production was performed using a planetary ball
91 mill with 5 mm zirconium oxide balls: 120 minutes at 450 rpm processes in 4 steps (10 cycles of 3

92 minutes of grinding and 6 minutes of a pause). A total organic carbon instrument (Shimadzu,
93 Kyoto, Japan) was used to determine the concentration of the dispersion. Characterization: 59
94 mg kg⁻¹ in concentration, DLS ($d_H = 310 \pm 10$ nm), zeta potential in pure water ($\zeta = -42.5 \pm 2.0$
95 mV), and transmission electronic microscopy (TEM) images given in supporting information (SI).

96
97 **Cigarette filter specifics.** Concerning the filters, two brands were used: “filter tip” from Rizla and
98 “filter tub” from Gizeh, named R and G, respectively. These filters are both composed of
99 hydrophilic cellulose acetate. For R and G, length = 16.0 and 15.0 mm, diameter = 6.0 and 8.0
100 mm, dry mass = 59.5 and 101.3 mg, dry mass per volume (density) = 131 and 134 mg/cm³, wet
101 mass = 412 and 828 mg, respectively. All the values are based on an average of measurements
102 on 20 filters.

103
104 **Instruments.** The AF4 system Eclipse 3+ AF4 instrument (Wyatt Technology, Dernbach,
105 Germany) with a 250- μ m channel thickness and a 10-kDa PES membrane, a 1200 series high-
106 performance liquid chromatography pump (Agilent Technologies, Les Ulis, France) equipped
107 with a UV-vis absorption detector (1200 series, Agilent Technologies, Les Ulis, France) and a
108 multiangle laser light scattering (MALS) detector (DAWN HELEOS, Wyatt Technology) has been
109 used. Data from the detectors were collected and analysed by ASTRA version 6 (Wyatt
110 Technology). The AF4 conditions for characterizing nanoplastics were previously optimized and
111 published (Gigault et al., 2017).

112
113 **Kinetic experiments:** Ten millilitres of dispersing media with 5 mg L⁻¹ NPTs was placed in a glass
114 vial, and then one CGB was introduced into the solution before gently stirring (orbital stirring,
115 100 RPM) the solution for a defined period of time. It should be noted that the CGB was

116 previously soaked in water to swell it. At time t , 2 mL of the medium was collected, filtered to
117 1.2 μm and injected into the AF4 apparatus. Blank preparations with no filters or NPTs were also
118 realized under the same conditions. Blanks with NPTs but without CGBs had a UV signal that
119 corresponded to $t=0$. Blanks with CGBs but without NPTs had no UV or MALS signals. All the
120 preparations were performed in triplicate at room temperature (25 ± 1 °C).

121 Use of the UV peak area (A_w) of the NPT dispersions from A4F-UV-SLS as a function of the
122 exposure time t allows to determine the total concentration of NPT in each solution (C_w) from
123 the residual fraction f . The latter is defined as follows: $f = A_w/A_{w0} = C_w/C_{w0}$, where A_{w0} and C_{w0}
124 are the peak area and the concentration of the initial NPT sample, respectively, based on the
125 mass in the aqueous medium. Experiments with known concentrations of PSLs (50, 180 and 500
126 nm) yielded $f = 0.009 \pm 0.001$ and $f = 0.003 \pm 0.001$ as the limits of quantification (LQ) and
127 detection (LD), respectively. Both types of NPT were mixed with CGBs in aqueous media, and
128 withdrawals of the supernatant were taken and analysed by an analytical method to determine
129 the potential interaction between CGBs and PSLs or NPTf.

130

131 **Sorption model:** The process governing the sorption of the NPT analyte is the overall result of
132 the competition between sorption and release. Fick's diffusion law quantifies this sorption
133 process, describes the exchange kinetics between cigarette butts and the aqueous phase, and
134 may be expressed as follows:

135
$$\frac{dC_s}{dt} = \frac{R_s}{V_s} \left(C_w - \frac{C_s}{K_{sw}} \right) \quad \text{equation 1}$$

136 where C_s and C_w are the NPT concentrations at time t in the CGBs and in water, respectively; V_s is
137 the CGB volume; R_s is the water sampling rate through the CGBs, which is linearly proportional
138 to the exchange surface of the filter; K_{sw} is the CGB-water partition coefficient defined as the

139 nanoplastics ratio in CGB and water (C_{CGB}/C_w); and the terms $R_S C_w/V_S$ and $R_S C_S/V_S K_{SW}$ are the
 140 expressions for sorption and release, respectively. The experiments correspond to a static
 141 exposure design in which the NPT concentration decreases with the exposure time. The solution
 142 of equation (1) is:

143

$$144 \quad f = \frac{C_w}{C_{w0}} = \frac{\left\{1 + \frac{K_{SW} V_S}{V_w} \exp\left[-\left(1 + \frac{K_{SW} V_S}{V_w}\right) \frac{R_S t}{K_{SW} V_S}\right]\right\}}{1 + \frac{K_{SW} V_S}{V_w}} \quad \text{equation 2}$$

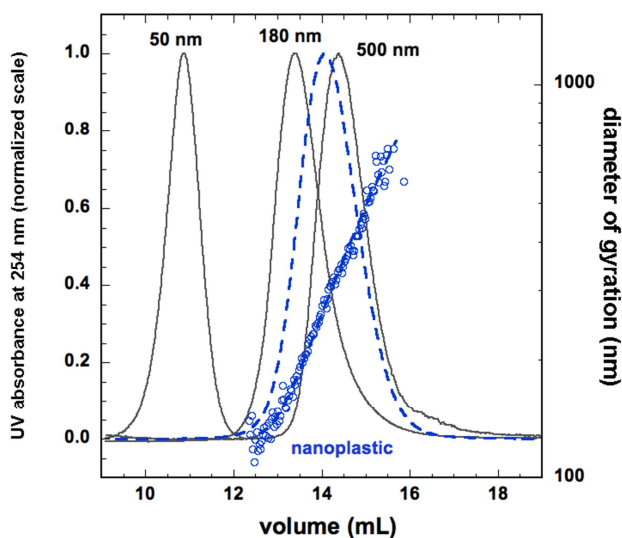
145 where V_w is the volume of the aqueous solution. In this model, for a simple case of exposure, it is
 146 assumed that (i) the rate of mass transfer to CGBs (receiving phase) is linearly proportional to
 147 the difference between the chemical activity of the contaminant (NPTs) in the water phase and
 148 that in CGBs; (ii) an equilibrium exists at the interface; and (iii) molecular diffusion is the
 149 predominant transport mechanism within CGBs with a diffusion coefficient that is time- and
 150 concentration-independent.

151 Results and discussion

152 **Sample characterization.** The hydrodynamic diameters (d_H) determined by dynamic light
 153 scattering (DLS) for the three PSLs batches are 50 ± 2 , 198 ± 10 , and 502 ± 30 nm, respectively,
 154 with ζ values in the range of -45 to -40 mV. NPTf presents an average d_H of (310 ± 10) nm, which
 155 is in the middle of the range of sizes for the PSL samples, and a ζ value in pure water of $(-42.5 \pm$
 156 $2.0)$ mV, which is in the range of values for the PSL samples. NPTf is polydisperse and
 157 polymorphic (Figure S1); indeed, the particle shape significantly deviates from those of the
 158 spherical monodisperse PSLs. The size distributions of both types of NPTs were compared by
 159 AF4-UV-SLS (Figure 1). The NPTf signal ranges from 13 to 16 mL, corresponding to sizes ranging
 160 from 180 nm to 800 nm in equivalent hydrodynamic diameter (based on retention volume). The

161 gyration diameter (d_g) of NPTf ranges from 100 to 800 nm, which confirms their size
162 polydispersity. The significant shift between d_H and d_g is another indication of the asymmetric
163 shape/structure of NPTf and has been explained elsewhere (Brewer and Striegel, 2011).

164



165

166 **Figure 1.** AF4-UV fractograms obtained for PSLs (50 nm, 180 and 500 nm) solutions, and NPTf solutions (blue dashed line)
167 with gyration diameter variation given by the MALS detector (blue open symbol).

168

169 **Particle influence.** Figure 2 shows the kinetics of the residual fraction f for PSLs (Figure 2a) and
170 NPTf (Figure 2b) in the presence of CGB-R and CGB-G in freshwater at room temperature and
171 under gentle agitation. It is worth mentioning that freshwater has been chosen because of the
172 lack of aggregation of NPTs in this medium, as opposed of the quick aggregation phenomenon
173 observed in a saline environment (critical coagulation concentration of approximately 25 g/L in
174 NaCl) (Schmitt et al., 2014). Within Figure 2, each time corresponds to one experiment
175 performed under the same triplicate conditions: one prehydrated filter at size equilibrium left in
176 10 mL of a 5 ppm nanoplastic solution. Under these conditions, the PSL residual fraction (f)
177 decreases rapidly within 0.5 hour to reach an equilibrium after 1 hour, and this behaviour seems
178 to be dependent on the PSL characteristics: the 500-nm PSL concentration decreases to a
179 residual fraction of $f = 0.1$, while the 50-nm PSL concentration decreases to $f = 0.01$. However,

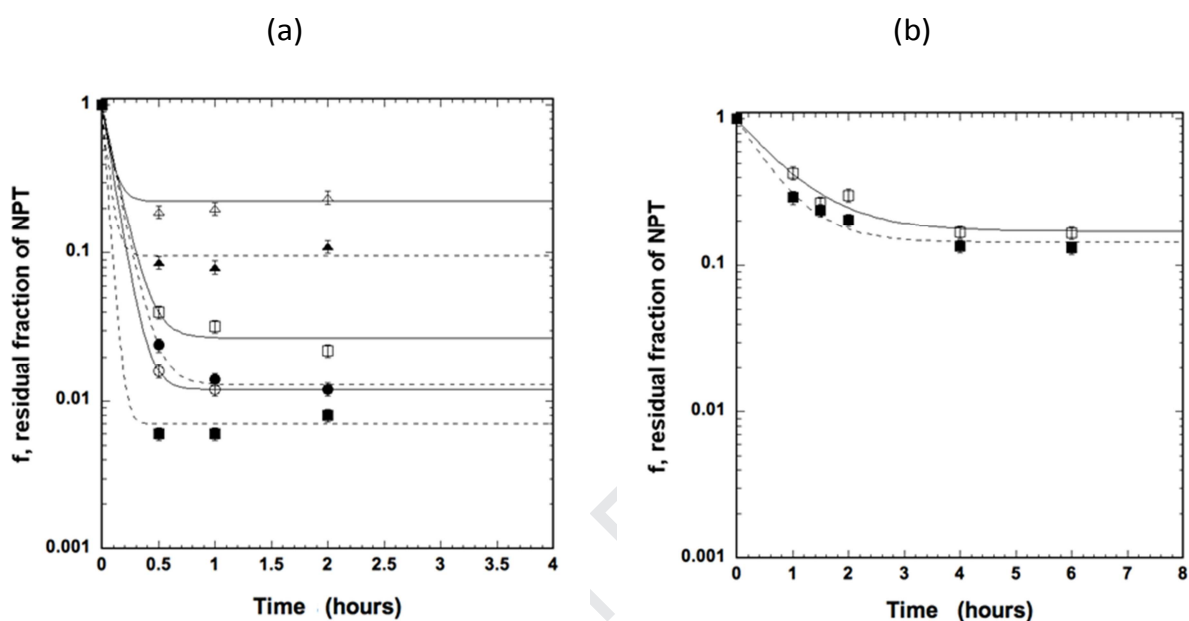
180 for the experimental conditions tested, no correlation was found between the size of the PSL
181 and the corresponding sorption kinetics, kinetic equilibrium is reached after 0.5 hours regardless
182 of the PSL size. A similar experiment was then performed by mixing both CGB-R and CGB-G with
183 an NPTf sample. Compared to the previous results, the residual fractions of the overall NPTf
184 sample at kinetic equilibrium are $f = 0.12$ and $f = 0.15$ for CGB-R and CGB-G, respectively. These
185 results, obtained for an NPTf sample exhibiting a continuum of sizes from 100 nm to 800 nm (see
186 Figure 1), are in accordance with the previous results obtained for PSLs of discrete sizes.
187 Nevertheless, kinetic equilibrium is reached after 4 hours, while equilibrium is reached after 1
188 hour regardless of the size of the PSL samples (see Figure 2a). Since NPTs have similar chemical
189 compositions and hydrodynamic size ranges, this difference could be attributed to the physical
190 properties of the nanoplastic batches, *i.e.*, PSLs versus NPTf. The longer equilibrium time of the
191 NPTf could be attributed to the difference in shape/structure as characterized by TEM (Figure
192 S1).

193
194 **Filter influence.** A small difference in sorption appears between the two filters, with slightly
195 higher NPT sorption on the CGB-R filter, and this phenomenon was more pronounced for the 50-
196 nm PSL. Both filters had the same densities (0.13 g/cm^3) and the same surface-to-volume ratios
197 (4.0). CGB-R was smaller in volume (0.45 and 0.75 cm^3 for CGB-R and CGB-G, respectively). These
198 comparisons suggest that the dimensional characteristics of the filters didn't explain the
199 influence of the filter on the sorption capacity, especially for highly diffusive species.

200 Whatever the characteristics, both filters present high sorption capacities for all the NPTs and
201 size ranges tested in this study.

202 It is interesting to compare the high sorption capacity for the 50-nm nanoplastics in freshwater
203 with the cut-off capacity observed on smoked cigarette butts. Indeed, Van Dirk et al.

204 demonstrated that nanoparticles with sizes ranging from 6 nm to 50 nm from cigarette smoke
 205 are generally transferred to humans, *i.e.*, not retained by the cigarette filter (van Dijk et al.,
 206 2011). Other studies showed that a smoked CGB releases soot particles larger than 70 nm into
 207 aqueous systems (Chevalier et al., 2018). There is a fairly remarkable difference in the abilities of
 208 filters to absorb nanoparticles in water versus air.



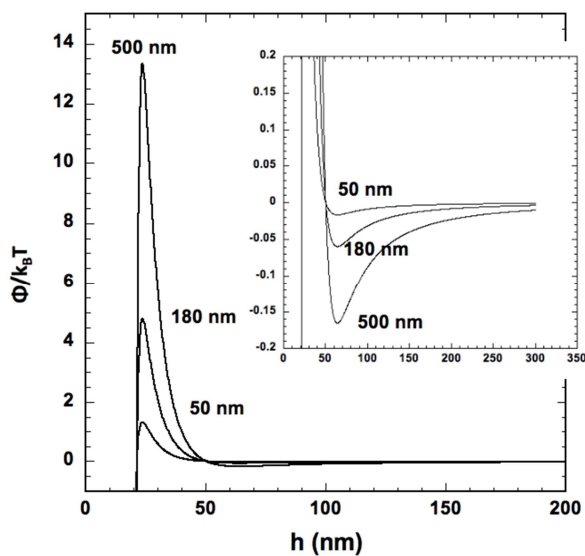
209 **Figure 2.** Sorption kinetics represented by the residual fraction (f) as a function of the contact time between CGBs (R is
 210 represented by closed symbols, and G is represented by open symbols) and a) PSL NPTs (50 nm (■□), 180 nm (●○) and 500
 211 nm (▲△)) or b) NPTf in solution. The initial concentration of NPTs was 5 mg L^{-1} . The lines correspond to the fit of the data
 212 based on the equation (2).

213

214

215 **Sorption mechanisms.** The sorption mechanisms of NPTs on carbon-based materials can be
 216 complex because electrostatic and nonelectrostatic interactions (depending on the absorbent,
 217 the absorbate and the solution chemistry) may come into play (Moreno-Castilla, 2004).
 218 Electrostatic interactions appear when charges (negative or positive) are involved. Figure 3
 219 presents XDLVO modelling (the conditions are summarized in the SI) according to the zeta
 220 potential of cellulose acetate and the different NPT batches used in the present study (Tadros,
 221 2013). The secondary minimum energy (insert in Figure 3) presents potentials favourable for

222 reaching the filter surface for all the NPTs. The more-retained 50 nm-PSL presents a less
223 favourable secondary energy minimum, and the less-retained 500 nm-PSL presents a more
224 favourable minimum. Usually, the secondary minimum does not affect the sorption kinetics.
225 However, when this minimum is deep enough, especially for larger particles, initial rapid
226 attachment may occur at the level of the secondary minimum (Trefalt and Borkovec, 2014). In
227 the investigation of the primary maximum energy, this tendency corresponds to the retention
228 behaviour. The lowest energy barrier is obtained for the 50 nm-PSL, and the highest barrier is
229 obtained for the 500 nm-PSL, which corresponds to the order experimentally observed for PSL in
230 Figure 3 and previously discussed. Under these conditions, XDLVO theory demonstrates that the
231 mechanisms allowing the retention of NPTs on the filter surface occur at a small separation
232 distance mostly for the 50 nm-PSL, where the energy barrier is the lowest for overcoming
233 electrostatic repulsion.



235
236 **Figure 3.** Potential curves of coagulation calculated by XDLVO theory for particles of various sizes.

237

238 **Sorption kinetics.**

239 Concerning the global capacity of CGB filters to retain nanoplastics in the environment, Table 1
 240 reports the K_{SW} values determined from equation 2. The results show partition coefficients
 241 within the range of 10^2 to 10^4 , reflecting a non-negligible bioaccumulation factor when
 242 considering CGBs in the food chain. Assuming an aquatic medium contaminated with 10 ppb of
 243 NPTs, as proposed within the literature, and the 750 000 metric tons of CGBs ending up as litter
 244 worldwide per year (Novotny et al., 2009), 0.75 to 75 metric tons of NPTs could be absorbed by
 245 cigarette filters each year. It is worth mentioning that NPTs are only one of the contaminants
 246 loaded within CGBs, as reported elsewhere (Chevalier et al., 2018). Many other contaminants,
 247 such as particles and metals, should be considered in used butts. Additionally, the partition
 248 coefficients determined for deionized water for the G-filter and 50-nm and 500-nm PSL are 8400
 249 and 890, respectively, slightly higher than those measured in freshwater (approximately 1.8-
 250 fold), demonstrating that the range of salinity of freshwater has little effect on the sorption of
 251 NPTs, compared to the values presented above.

252

253 **Table 1:** water sampling rate R_s and CGB-water partition coefficient K_{sw} determined by adjusting the kinetic curves
 254 (Figure 2). The curve fit based on the Levenberg-Marquardt algorithm was calculated using an iterative procedure
 255 on equation 2.

256

Sample	z-average (nm)	R_s (mL/min)		K_{sw}	
		G	R	G	R
PSL	50	96	100*	4450	24000*
PSL	180	108	175	12370	16600
PSL	500	107	150	520	1840
NPTf	310	10	17	710	1380

261

* with $f < LOQ$

262 In Table 1, the differences between the R_s values obtained for CGB-G and CGB-R are due to the
 263 calculation method (see Equation (2)) based only on the CGB external dimensions and not the
 264 porosity. The surface area ratio between CGB-G and CGB-R is 0.7, while the corresponding R_s

265 ratio is 0.6-0.7. Furthermore, the R_s values are significantly different for PSLs and NPT f , with a
266 value one order of magnitude lower for the latter. All other things being equal, R_s depends on
267 the diffusion coefficient of NPTs in CGB through the overall mass transfer coefficient, k_0 . The
268 NPT f sample has an intermediate diffusion coefficient compared to those of 180-nm PSL and
269 500-nm PSL, as shown by the results reported in Figure 2. Based on these results, the filter
270 nature (*i.e.* R or G) has negligible contribution to sorption capacity rather than the size and
271 morphology of nanoplastics. More specifically, the anisotropy of the NPT f sample may be what
272 strongly affects its diffusion coefficient in CGBs.

273 Unfortunately, quantitative experiments on used butts could not be carried out with the
274 analytical methodology proposed in this work. Used CGBs release organic matter, including a
275 nanoparticulate fraction that strongly interferes with the results of AF4 analysis. However, from
276 a qualitative point of view and as illustrated within the graphical abstract, a 20-ppm water
277 solution of blue coloured PSL 200 nm quickly turns colourless when either an unused or used
278 CGB is added. The exposure concentrations and times are similar to those of the experiment
279 using an unused CGB as described above. This qualitative result reinforces the idea of similar
280 strong NPT sorption on both unused and used CGBs.

281

282 **Conclusions**

283 In this work, we addressed the problem of the behaviour of nanoplastics (NPTs) in the
284 environment through a better understanding of their interaction with one of the most
285 predominant types of waste: cigarette butts. We also demonstrated the high capacity of NPTs to
286 be absorbed on cigarette butts. A quantitative kinetic approach was used to evaluate the
287 partition coefficients between NPTs and CGBs, which ranged from 10^2 to 10^4 at room

288 temperature in freshwater. These strong partition coefficients suggest that NPTs present in the
289 environment may be transferred to porous organic matrices. The determination of the water
290 sampling rate demonstrates the significant effect of nanoplastic morphology on the sorption
291 behaviour. Nanoplastics prepared by mechanical fragmentation with high size polydispersity and
292 anisotropic morphology exhibit diffusion coefficients in butts that differ from those obtained for
293 NPTs with spherical morphologies such as PSLs. This result also demonstrates the importance of
294 taking into consideration the morphology of nanoplastic samples when determining the
295 mechanisms that govern the transfer, accumulation and fate of NPTs.

296 **Conflicts of interest**

297 There are no conflicts of interest to declare.

298 **Acknowledgements**

299 This research was carried out under the framework of E2S UPPA supported by the
300 “Investissements d'Avenir” French programme managed by ANR (ANR-16-IDEX-0002).

301 **Notes and references**

- 302 Alimi, O.S., Farner Budarz, J., Hernandez, L.M., Tufenkji, N., 2018. Microplastics and Nanoplastics in
303 Aquatic Environments: Aggregation, Deposition, and Enhanced Contaminant Transport. *Environ.*
304 *Sci. Technol.* 52, 1704–1724. <https://doi.org/10.1021/acs.est.7b05559>
- 305 Araújo, M.C.B., Costa, M.F., 2019. A critical review of the issue of cigarette butt pollution in coastal
306 environments. *Environ. Res.* 172, 137–149. <https://doi.org/10.1016/j.envres.2019.02.005>
- 307 Brewer, A.K., Striegel, A.M., 2011. Characterizing String-of-Pearls Colloidal Silica by Multidetector
308 Hydrodynamic Chromatography and Comparison to Multidetector Size-Exclusion
309 Chromatography, Off-Line Multiangle Static Light Scattering, and Transmission Electron
310 Microscopy. *Anal. Chem.* 83, 3068–3075. <https://doi.org/10.1021/ac103314c>
- 311 Chevalier, Q., El Hadri, H., Petitjean, P., Bouhnik-Le Coz, M., Reynaud, S., Grassl, B., Gigault, J., 2018.
312 Nano-litter from cigarette butts: Environmental implications and urgent consideration.
313 *Chemosphere* 194, 125–130. <https://doi.org/10.1016/j.chemosphere.2017.11.158>
- 314 da Costa, J.P., Santos, P.S.M., Duarte, A.C., Rocha-Santos, T., 2016. (Nano)plastics in the environment –
315 Sources, fates and effects. *Sci. Total Environ.* 566–567, 15–26.
316 <https://doi.org/10.1016/j.scitotenv.2016.05.041>

317 Davranche, M., Veclin, C., Pierson-Wickmann, A.-C., El Hadri, H., Grassl, B., Roweczyk, L., Dia, A., Ter
318 Halle, A., Blanco, F., Reynaud, S., Gigault, J., 2019. Are nanoplastics able to bind significant
319 amount of metals? The lead example. *Environ. Pollut.* 249, 940–948.
320 <https://doi.org/10.1016/j.envpol.2019.03.087>

321 Dong, Z., Zhu, L., Zhang, W., Huang, R., Lv, X., Jing, X., Yang, Z., Wang, J., Qiu, Y., 2019. Role of surface
322 functionalities of nanoplastics on their transport in seawater-saturated sea sand. *Environ. Pollut.*
323 255, 113177. <https://doi.org/10.1016/j.envpol.2019.113177>

324 El Hadri, H., Gigault, J., Maxit, B., Grassl, B., Reynaud, S., 2020. Nanoplastic from mechanically degraded
325 primary and secondary microplastics for environmental assessments. *NanoImpact* 17.
326 <https://doi.org/10.1016/j.impact.2019.100206>

327 Gigault, J., El, H., Reynaud, S., Deniau, E., Grassl, B., 2017. Asymmetrical flow field flow fractionation
328 methods to characterize submicron particles: application to carbon-based aggregates and
329 nanoplastics. *Anal. Bioanal. Chem.* 409, 6761–6769. <https://doi.org/10.1007/s00216-017-0629-7>

330 Gigault, J., Pedrono, B., Maxit, B., Halle, A.T., 2016. Marine plastic litter: the unanalyzed nano-fraction.
331 *Environ. Sci.: Nano* 3, 346–350. <https://doi.org/10.1039/C6EN00008H>

332 Gillibert, R., Balakrishnan, G., Deshoules, Q., Tardivel, M., Magazzù, A., Donato, M.G., Maragò, O.M.,
333 Lamy de La Chapelle, M., Colas, F., Lagarde, F., Gucciardi, P.G., 2019. Raman Tweezers for Small
334 Microplastics and Nanoplastics Identification in Seawater. *Environ. Sci. Technol.* 53, 9003–9013.
335 <https://doi.org/10.1021/acs.est.9b03105>

336 Hartmann, N.B., Hüffer, T., Thompson, R.C., Hassellöv, M., Verschoor, A., Dugaard, A.E., Rist, S.,
337 Karlsson, T., Brennholt, N., Cole, M., Herrling, M.P., Hess, M.C., Ivleva, N.P., Lusher, A.L., Wagner,
338 M., 2019. Are We Speaking the Same Language? Recommendations for a Definition and
339 Categorization Framework for Plastic Debris. *Environ. Sci. Technol.* 53, 1039–1047.
340 <https://doi.org/10.1021/acs.est.8b05297>

341 Hengstberger, M., Stark, M., 2009. Fibre and Particle Release from Cigarette Filters. *Beitr. Zur Tab. Int.*
342 *Tob. Res.* 23, 338–358. <https://doi.org/10.2478/cttr-2013-0869>

343 Lambert, S., Wagner, M., 2016a. Characterisation of nanoplastics during the degradation of polystyrene.
344 *Chemosphere* 145, 265–268. <https://doi.org/10.1016/j.chemosphere.2015.11.078>

345 Lambert, S., Wagner, M., 2016b. Formation of microscopic particles during the degradation of different
346 polymers. *Chemosphere* 161, 510–517. <https://doi.org/10.1016/j.chemosphere.2016.07.042>

347 Li, P., Li, Q., Hao, Z., Yu, S., Liu, J., 2020. Analytical methods and environmental processes of
348 nanoplastics. *J. Environ. Sci.* 94, 88–99. <https://doi.org/10.1016/j.jes.2020.03.057>

349 Mackay, J., Eriksen, M., Eriksen, M.P., 2002. The tobacco atlas. World Health Organization.

350 Moreno-Castilla, C., 2004. Adsorption of organic molecules from aqueous solutions on carbon materials.
351 *Carbon* 42, 83–94. <https://doi.org/10.1016/j.carbon.2003.09.022>

352 Novotny, T., Lum, K., Smith, E., Wang, V., Barnes, R., 2009. Cigarettes Butts and the Case for an
353 Environmental Policy on Hazardous Cigarette Waste. *Int. J. Environ. Res. Public Health* 6, 1691–
354 1705. <https://doi.org/10.3390/ijerph6051691>

355 Novotny, T.E., Slaughter, E., 2014. Tobacco Product Waste: An Environmental Approach to Reduce
356 Tobacco Consumption. *Curr. Environ. Health Rep.* 1, 208–216. <https://doi.org/10.1007/s40572-014-0016-x>

357

358 Pessoni, L., Veclin, C., El Hadri, H., Cugnet, C., Davranche, M., Pierson-Wickmann, A.-C., Gigault, J.,
359 Grassl, B., Reynaud, S. (2019) Soap- and metal-free polystyrene latex particles as a nanoplastic
360 model. *Environmental Science: Nano*. 6, 2253-2258.

361 Pikuda, O., Xu, E.G., Berk, D., Tufenkji, N., 2018. Toxicity Assessments of Micro- and Nanoplastics Can Be
362 Confounded by Preservatives in Commercial Formulations. *Environ. Sci. Technol. Lett.* 6, 21–25.
363 <https://doi.org/10.1021/acs.estlett.8b00614>

- 364 Pu, D., Kou, Y., Zhang, L., Liu, B., Zhu, W., Zhu, L., Duan, T., 2019. Waste cigarette filters: activated
365 carbon as a novel sorbent for uranium removal. *J. Radioanal. Nucl. Chem.* 320, 725–731.
366 <https://doi.org/10.1007/s10967-019-06502-z>
- 367 Schmitt, C., Grassl, B., Lespes, G., Desbrières, J., Pellerin, V., Reynaud, S., Gigault, J., Hackley, V.A., 2014.
368 Saponins: A Renewable and Biodegradable Surfactant From Its Microwave-Assisted Extraction to
369 the Synthesis of Monodisperse Lattices. *Biomacromolecules* 140131113511009.
370 <https://doi.org/10.1021/bm401708m>
- 371 Shen, M., Zhang, Y., Zhu, Y., Song, B., Zeng, G., Hu, D., Wen, X., Ren, X., 2019. Recent advances in
372 toxicological research of nanoplastics in the environment: A review. *Environ. Pollut.* 252, 511–
373 521.
- 374 Tadros, T., 2013. Elastic Repulsion, in: Tadros, T. (Ed.), *Encyclopedia of Colloid and Interface Science*.
375 Springer Berlin Heidelberg, Berlin, Heidelberg, pp. 341–341. [https://doi.org/10.1007/978-3-642-
376 20665-8_73](https://doi.org/10.1007/978-3-642-20665-8_73)
- 377 Trefalt, G., Borkovec, M., 2014. Overview of DLVO theory. *Lab. Colloid Surf. Chem. Univ. Geneva* 29.
- 378 van Dijk, W.D., Gopal, S., Scheepers, P.T.J., 2011. Nanoparticles in cigarette smoke; real-time undiluted
379 measurements by a scanning mobility particle sizer. *Anal. Bioanal. Chem.* 399, 3573–3578.
380 <https://doi.org/10.1007/s00216-011-4701-4>
- 381 Wagner, S., Reemtsma, T., 2019. Things we know and don't know about nanoplastic in the environment.
382 *Nat. Nanotechnol.* 14, 300–301. <https://doi.org/10.1038/s41565-019-0424-z>

Fate of nanoplastics in the environment: implication of the cigarette butts

Hind El Hadri, Jesus Maza Lisa, Julien Gigault, Stéphanie Reynaud, Bruno Grassl

Highlights:

- The nanoplastic sorption by cigarette filters was evaluated in pure and freshwater
- The sorption was addressed for nanoplastics of various morphologies and dispersity.
- A kinetic approach gives cigarette filters partition coefficient within 10^2 - 10^4

Author statements

Dr. Hind El Hadri: methodology, investigation, writing

Dr. Jesus Maza-Lisa: methodology, investigation

Dr. Julien Gigault: Supervision, investigation, writing

Dr. Stéphanie Reynaud: Supervision, Resources, writing

Prof Bruno Grassl: Supervision, Resources, writing

Journal Pre-proof